

Axial Breakdown In Linear And Disk MHD Generators

Author(s): W. Unkel, G.Tesfaye, and J. D. Teare

Session Name: Disk Generators

SEAM: 19 (1981)

SEAM EDX URL: <https://edx.netl.doe.gov/dataset/seam-19>

EDX Paper ID: 855

Axial Breakdown in Linear and Disk MHD Generators

W. Unkel, G. Tesfaye and J.D. Teare
 Energy Laboratory and Department of Mechanical Engineering
 Massachusetts Institute of Technology
 Cambridge, Massachusetts 02139

Abstract

A new inter-electrode insulator designed to prevent insulator-induced axial breakdown has been tested under conditions of applied electric field. The design was successful in its main goal; however, indications are that the plasma breakdown threshold voltage was somewhat compromised by the design. Some preliminary measurements of breakdown thresholds relevant to disk generators are also presented. A previously developed analytical model of axial breakdown has been improved and preliminary results indicate the importance of electron temperature elevation and confirm the need to consider electron recombination with a heavy particle as the third-body.

Introduction

Previous experimental and analytical work has characterized and quantified many of the aspects of axial breakdown in linear MHD generators [1, 2, 3, 4]. In particular, results for a simplified electrode configuration have shown that a threshold voltage must be exceeded and that breakdown can be initiated either by the plasma or by the inter-electrode insulator itself. For many electrode wall designs, the threshold voltage for insulator-initiated breakdown is lower than that for plasma breakdown; some improvement in generator performance might be achieved if insulator-initiated breakdown can be prevented. Plasma-initiated and insulator-initiated threshold voltages have been calculated for a simplified, applied field configuration [2, 4]. A two dimensional, time-dependent computer solution was used to solve the coupled fluid and electrical problem for the plasma; the plasma solution was coupled to a thermal and electrical solution for the inter-electrode insulator. The results compared favorably with the measured response, but the effect of Joule heating in the plasma was generally under-predicted. The first part of this paper presents experimental results for an inter-electrode wall configuration designed to prevent insulator-initiated breakdown. Some improvements to the two-dimensional plasma code are described and results presented for the axial configuration.

The disk generator has been advanced as an alternate generator configuration, with one possible advantage that breakdown problems will be eliminated or reduced. Plasma breakdown threshold voltages have been calculated by Shamma [5]; however, there are some aspects not considered in his model and there is need for additional modeling and perhaps even more for experimental data. The second part of the paper addresses the general problem of breakdown for disk generators. A simplified configuration, which simulates some of the characteristics of a disk generator, is considered using a modified version of the breakdown code discussed above. A very limited set of experimental results is also presented for this configuration.

Laminated Inter-Electrode Insulator Design

Experimental and analytical results of Unkel

[1] implied that insulator-initiated breakdown could be prevented by careful thermal design of the inter-electrode wall components; some results of Hermina [3] confirm this. The present work studied a "laminated" insulator design (see Fig. 1) which provides the necessary cooling in the regions of high Joule heating, but which keeps the average surface temperature as high as possible. In this design, two cooled metallic pieces are placed next to thin insulators which are adjacent to the electrodes; a wide insulator separates the two cooled metallic pieces.

Thermal Analysis. An approximate plasma side convection and wall side heat conduction model was developed to help design the wall such that breakdown would not be initiated by the insulator. The heat transfer from a turbulent boundary layer to a wall with a prescribed variation of surface temperature was developed following the method of Kays [6]. Previously calculated increases in heat flux resulting from Joule heating were incorporated into the calculation procedure. A quasi-two-dimensional solution, including axial conduction between the components through a specified contact resistance, was obtained for the composite wall.

The main parameters which can be controlled in the design are the inter-electrode insulator materials and the degree of cooling of the metallic components. The cooling of the metal components is adjusted by changing the thickness of a stainless-steel cap brazed to a water cooled copper backing piece. The most important parameter not easily controlled is the contact resistance between the ceramic insulators and the water-cooled metallic elements. A design with alumina for the thin insulators was first considered and the resulting wall temperature distribution is shown in Fig. 2. The electrode was designed to operate at a uniform temperature of 1100 K in the absence of Joule heating and the "cooler" piece was constructed entirely of copper to provide the maximum cooling of the alumina insulator. The large insulator was MgO and the contact of the MgO with the surrounding copper was assumed to be good. The wall temperature distribution with a plasma current of 35 amps (typical of the level required to produce plasma-initiated breakdown) is compared, in Fig. 2, with the distribution with no current. Significant increases in the electrode temperature and more importantly in the alumina temperature make this design unacceptable. Even when additional cooling was provided to the electrode, the thermal design was still unacceptable. The final design used boron-nitride for the insulators adjacent to the electrodes and was designed to have the electrodes operate at a uniform temperature of 1100 K, with a current of 35 amps flowing through the plasma. The cooler pieces were stainless-steel capped copper designed to keep the boron-nitride temperature at approximately 1200 K with a 35 ampere current. The contact between the MgO and the surrounding cooling pieces was assumed to be poor, such that the surface temperature would be high. The calculated temperature distributions with and without current are shown in Fig. 3; the insulator temperatures

appear to be below the levels for which insulator-initiated breakdown would be expected.

Experimental Set-up. The inter-electrode configuration discussed above was assembled and tested under an applied electric field in the M.I.T. MHD Simulation Facility [7]. The basic plasma conditions of the tests were:

$$\dot{m} = 0.18 \text{ kg/s}$$

$$u = 4.08 \text{ m/s}$$

$$T_{\text{plasma}} = 2590 \text{ K}$$

$$\sigma \approx 6.8 \text{ mho/m.}$$

The basic experimental set-up is shown in Fig. 1; the details of the electrode module construction are shown in Fig. 4. A window port was installed on the wall opposite the electrode module to allow visual observations. A dual filter video recorder system was used to record separate images of the plasma and wall response. Voltage probes were inserted in the near-electrode region to measure the response of the voltage drops; the potentials of the cooler pieces were also measured. The axial voltage was supplied by two HP-6479C solid-state power supplies, together capable of operating at 600 volts and 35 amps. The voltage and current control circuitry of the power supplies was such that momentary (~0.1 sec) levels of high current were possible, but such that steady arcs in excess of 35 amps were not allowed; this characteristic was useful in minimizing damage from the arcs which were formed.

Experimental Results.

The main experimental results were obtained by applying successively higher voltages between the electrodes until breakdown was observed. Experiments were performed for three configurations:

- a) upstream electrode as an anode;
- b) upstream electrode as a cathode; and
- c) upstream electrode as an anode and the cooler pieces shorted together. The total voltage versus axial current variations for each of the three cases are shown in Fig. 4a-4c. As indicated in the figures, breakdown was observed for each configuration. The dual filter video records indicated that all breakdowns were initiated by the plasma. Several different types of breakdown were observed and will be discussed below. The plasma-initiated threshold voltage for configurations a and b was approximately 210 volts for a 2.0 cm total gap; this compares with a level of ~240 to 270 volts for a 1.91 cm monolithic MgO insulator as measured in previous experiments at Stanford. The plasma conditions are somewhat different, but it appears that the plasma breakdown strength may have been compromised by the addition of the intermediate metal cooling pieces.

Results With the Cooler Pieces Unshorted. The potentials of the cooler pieces and the electrode pieces are shown in Fig. 5 for the pre-breakdown condition and for two types of breakdown. Prior to breakdown the majority of the overall voltage drop is in the regions near the anode and cathode. In some cases the breakdown was partial, in that one or both of the gaps near the main electrodes arced, but no strong discharge was observed in the region over the MgO insulator; the resulting voltage distribution is shown in the figure. This type of breakdown occurred when the voltage dif-

ference was ~80 volts for the upstream gap and ~100 volts for the downstream gap; breakdown was observed once at the upstream gap with a voltage of 50 volts. After breakdown a voltage of ~110 volts was applied across the center 8mm MgO insulator. Previous data indicate a plasma breakdown voltage of 170 volts and an insulator breakdown voltage of 110 volts for this size gap; unfortunately, the quenching of the arcs by the power supply did not allow us to see if insulator breakdown of the 8mm gap would have followed. For other applications of voltage, the center was also bridged by a breakdown arc and the resulting distribution is shown in Fig. 5. The video records showed that the upstream gap was arcing and that an arc had formed between the upstream cooler piece and the downstream electrode. The arc bridging the upstream gap covered a significant width of the electrode (or was rapidly moving laterally) and the current was considerably higher than when only the two small gaps were bridged by arcs.

Results With the Cooler Pieces Shorted. The formation of arcs between the various metallic segments requires additional voltage drops to be established on the elements which are not directly supplied by the power source. To obtain some information on the effect that these extra voltage drops have on the breakdown behavior, the two cooler pieces were externally shorted and the resulting configuration tested. As indicated in Fig. 4, breakdown was observed at considerably lower voltages; in one instance at 125 volts. These breakdowns were considerably more intense than the partial breakdowns observed when the cooler pieces were unshorted. The voltage differences between the gaps when breakdown occurred were ~50 volts for the upstream gap and ~75 volts for the downstream gap; these compare to levels of 80 to 100 volts when the pieces were not shorted.

Breakdown Phenomena in Disk Generators

With the exception of the main current take-offs (and intermediate current taps if necessary) the walls of the disk generator are insulator walls, that is, they are designed to carry no net current. This configuration is considered to be favorable for prevention of axial breakdown and it is generally felt that higher axial fields can be accommodated for disk generators. Although it is possible that large size totally ceramic walls may be developed for the disk generator, it is more likely that the walls will be composed of alternating insulating and conducting rings as shown schematically in Fig. 6. Although the rings cause no distortion in the azimuthal direction, the local shorting in the radial direction can lead to circulating currents as shown in the figure. Considering regions away from the current-conducting electrodes, the disk generator can be assumed to have the following advantages relating to the breakdown threshold voltage:

- a) since the metallic conductors do not normally carry current, the voltage drop due to the electrode mechanisms must be supplied out of the per pair voltage difference.
- b) since the wall is perpendicular to the magnetic field the current concentrations around the electrode edges are not as severe as near linear generator inter-electrode gaps.

In addition, if breakdown occurs, the disk configuration may be less prone to damage, as the $J \times B$ forces on the resulting arc would be in the plane of the wall, rather than into the wall, as on the anode side of a linear generator.

Some breakdown threshold voltage calculations have been performed by Shamma [5]; however, additional calculations and measurements of breakdown characteristics are desirable.

Experimental Simulation of Disk Generator Breakdown. As a first step in providing a data base for disk generator breakdown, a channel with the electrode arrangement shown in Fig. 6 was designed and assembled. An axial field is applied to the simulated disk wall by driving current axially down the channel from the upstream electrode pair to the downstream electrode pair. A window port is provided to allow a full view of the simulated disk wall and voltage probes are mounted at various locations near the test module. The electrodes of the test module were designed in a manner similar to that of the linear breakdown module. The insulator is a 1/4" MgO insulator.

The experiment was assembled, but only limited results were obtained because of electrical shorting of the electrodes used to apply the axial field interior to the channel walls (i.e., not through the plasma). The highest voltage difference between the simulated disk wall elements was ~60 volts, at which point arc spot activity was observed on the upstream electrode element.

The gap between adjacent electrodes was tested under applied field conditions and plasma-initiated breakdown was observed at a voltage of 130 volts. For this gap of 6.4 mm a plasma breakdown threshold voltage of 150 to 170 volts is indicated from previous data.

Plasma Breakdown for Axial and Simulated Disk Configurations

The coupled fluid and electrical model for the axial discharge configuration, originally developed at Stanford [1], has been improved and extended to consider additional electrode configurations including the simulated disk configuration. The time-dependent fluid solution is obtained for a two-dimensional flow region using the usual boundary layer assumptions; the current distribution is calculated for the same two dimensional region. The original code solved the electron continuity equation using the three body electron reaction rates of Curry [8]; using these rates considerable departure from the equilibrium electron number density was observed in the boundary layer. The work of Okazaki [9] points out the need to consider three body heavy recombination especially at the lower temperatures; further examination of the literature indicates that recombination rates with N_2 as the third body [10] are faster even than the rates for CO_2 used by Okazaki. With the electron number density maintained close to equilibrium, the assumption of $T_e \approx T_g$ made in the initial work will be violated at lower currents and electron temperature non-equilibrium has been included in the code.

Calculations were made for conditions close to those in the disk breakdown experiment. A first set of calculations was made for an axial dis-

charge and a second set was made for the simulated disk configuration. The voltage current characteristic for the axial discharge is shown in Fig. 7 for the calculation where a balance between Joule heating and inelastic collisional losses is used to determine T_e (an inelastic loss factor of 1000 times the elastic rate was assumed) and also for a case where T_e is forced to remain close to the gas temperature. As can be observed, the electron temperature elevation significantly reduces the axial voltage and indicates that breakdown will occur at a significantly lower voltage and current than would be predicted with the electron temperature equal to the gas temperature; also in the case with $T_e \approx T_g$ the breakdown occurs closer to the wall. Even with the faster rates, in the axial configuration the rapid change in wall temperature (as the gas flows from the brick to the electrode) causes the electron number density to be above the equilibrium values in the region close to the electrodes. The work of Martinez [11] indicates that a secondary ionization layer forms near the wall due to high T_e and greatly accelerated ionization by electron impact. The high values of n_e near the wall in the absence of Joule heating result in low dissipation at a given current level and therefore may delay the formation of this layer; nonetheless this process will occur and it should be considered in more detail for the axial configuration.

For comparison, calculations were also made for the simulated disk configuration and the results are shown in Fig. 7; the voltage between the simulated electrodes is plotted against the current flow through an electrode (net current to these elements is zero). No "extra" cathode voltage drop is included in the calculations. A threshold voltage of ~160 volts is indicated for this 6.4 mm gap in the disk configuration in contrast to a level of ~180 for the direct axial applied field. It should be pointed out that the alternating metal/ceramic ring configuration is only one of several concepts examined for disk fabrication. More detailed evaluation of these concepts is clearly required.

Summary and Conclusions

The experimental results of applied field testing of a laminated inter-electrode insulator wall have been presented. The design was successful in avoiding insulator-initiated breakdown; however, the exposed metallic elements appeared to compromise the resistance to plasma breakdown. In most cases arcing was observed between the main electrode and the intermediate metallic cooling pieces rather than an arc spanning the entire gap between the main electrodes. An initial experiment to study breakdown phenomena in disk generators with walls constructed of metallic rings separated by insulator was run; however, only moderate voltages (60 volts) were applied and no breakdown was observed (or expected). The theoretical model to predict plasma breakdown, originally developed at Stanford, has been improved to consider electron-temperature non-equilibrium and to use three-body heavy recombination rates in addition to the three-body electron rates. The results for the applied field geometry show that electron temperature elevation leads to a reduction in the threshold voltage, and a change in the distance from the

wall at which the breakdown develops. Further analytical work should be addressed to this problem and additional comparisons with measurements of breakdown should be made.

Acknowledgment

This work was supported by the United States Department of Energy under Contract DE-AC01-79 ET 15518.

References

- 1 Unkel, W. and Kruger, C.H., "Axial Field Limitations in MHD Generators," Proceedings of the 16th Symposium on Engineering Aspects of Magnetohydrodynamics, Pittsburgh, PA, 1977.
- 2 Unkel, W. "Axial Field Limitations in MHD Generators," Topical Report prepared for U.S. D.O.E., FE-2341-8, April 1978.
- 3 Hermina, W. and Kruger, C.H., "Interelectrode Insulator Performance Under an Applied Field," 7th International Conference on MHD Electrical Power Generation, M.I.T., Cambridge, MA, June 1980.
- 4 Oliver, D.A., "The Prediction of Inter-electrode Breakdown in Magnetohydrodynamic Generators," M.I.T. GTL Report #116, March 1974.
- 5 Shamma, S., Martinez-Sanchez, M. and Louis, J.F., "Electric Effects of Boundary Layers and Breakdown on the Side Walls of Disk MHD Generators," Paper AIAA-80-1342, Presented at AIAA 13th Fluid and Plasma Dynamics Conference, Snowmass, Colorado, July 1980.
- 6 Kays, W.M., "Convective Heat and Mass Transfer," McGraw-Hill, Inc., 1966.
- 7 Zipursky, H.J., "Electrical Conductivity and Temperature of Plasmas in MHD Ducts," M.S. Thesis, M.I.T., September 1978.
- 8 Curry, W.P., "Collisional Radiative Recombination in Hydrogen Plasmas and in Alkali Plasmas," Physical Review A, 1, 1970.
- 9 Okazaki, K. et al, "Analysis of the Seeded Combustion Gas Boundary Layer Near a Cold Electrode," AIAA Journal, 15, pp 1778-1784, 1977.
- 10 Mansbach, P. and Sutton, E.A., Private Communication, 1977.
- 11 Martinez-Sanchez, M., et al, "Electron-Induced Reaction Rates in the Immediate Vicinity of Anodes," Proceedings of the Seventeenth International Conference on MHD Power Generation, M.I.T., Cambridge, MA, June 1980.

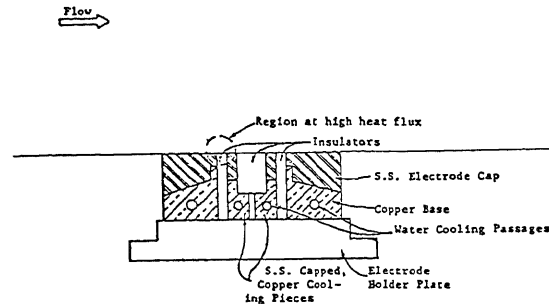
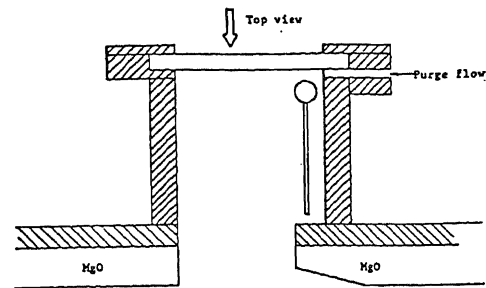


Figure 1. Schematic of Laminated Inter-electrode Insulator Module and Experimental Configuration used for Applied Field.

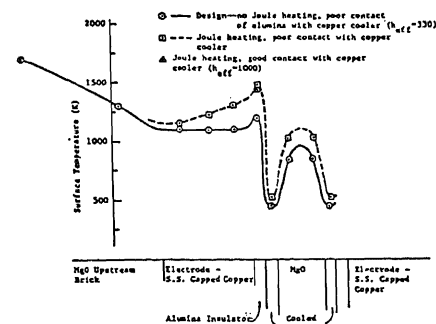


Figure 2. Wall Temperature Distribution for Laminated Electrode Design Using Alumina. Wall Components Designed to Give the Shown Distribution in the Absence of Joule Heating.

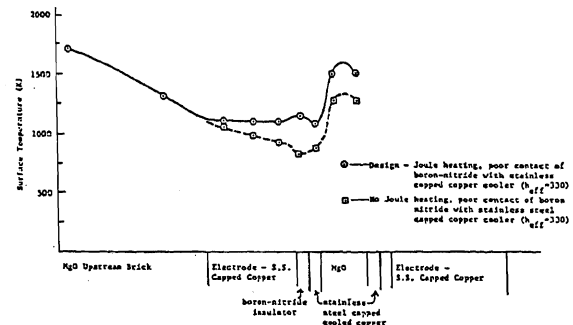


Figure 3. Wall Temperature Distribution for Laminated Electrode Design Using Boron-Nitride. Wall Components Designed to give the desired Temperature Distribution with Joule Heating.

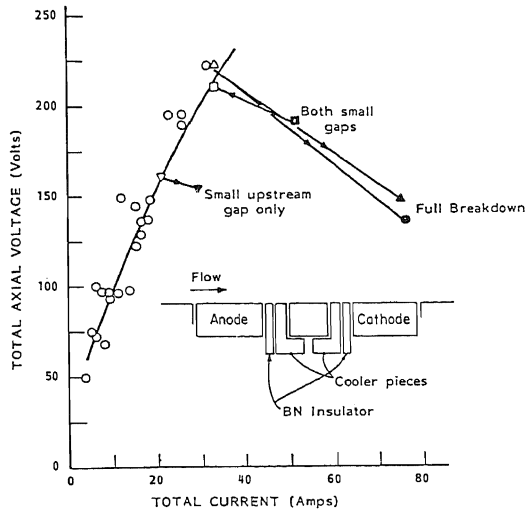


Figure 4a. Plot of Total Axial Voltage Versus Total Axial Current Showing Pre-breakdown and Post-Breakdown Conditions. Anode was Upstream Electrode and "Cooler" Pieces Were Unshorted.

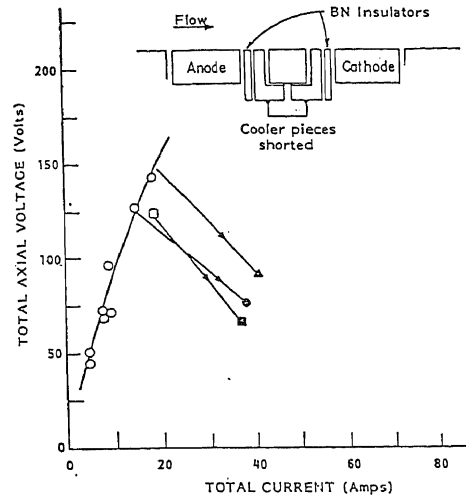


Figure 4c. Plot of Total Axial Voltage Versus Total Axial Current Showing Pre-breakdown and Post-Breakdown Conditions. All Breakdowns Were Plasma Initiated. Anode was the Upstream Electrode and the Cooler Pieces were Shorted Out. The Breakdowns Spanned Both Small Gaps.

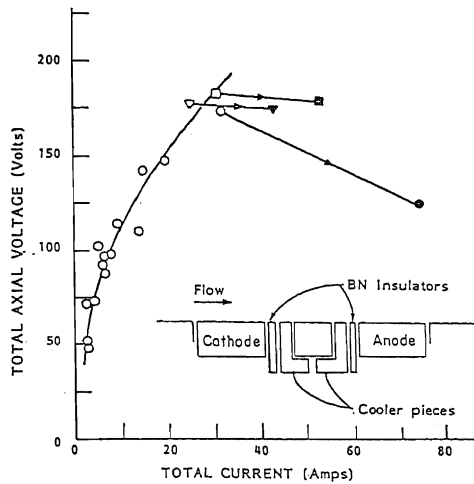


Figure 4b. Plot of Total Axial Voltage Versus Total Axial Current Showing Pre-breakdown Conditions. All Breakdowns were Plasma Initiated, but Not All Spanned the Entire Inter-Electrode Gap. Cathode was the Upstream Electrode and the "Cooler" Pieces were Unshorted.

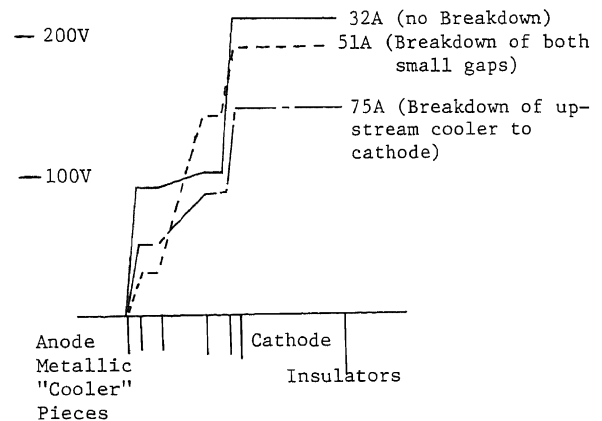


Figure 5. Potentials of electrode module components for no breakdown and for two types of breakdown.

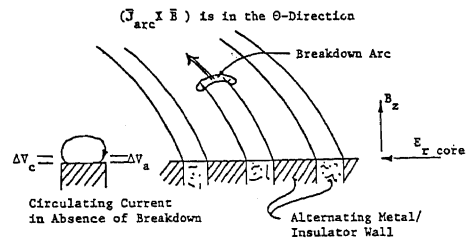


Figure 6. Schematic of the Disk Generator Wall Away from Electrode Current Take-offs.

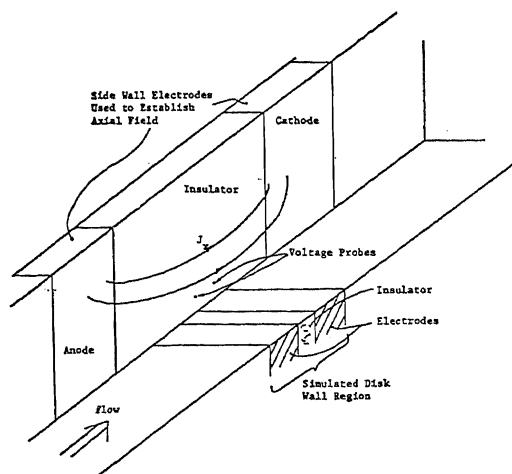


Figure 7. Sketch of Channel Configuration Used to Simulate the Disk Generator. Electrodes on Both Sidewalls are Used to Apply an Axial Field Across the Simulated Disk Wall. Optical Access is Provided to take Dual Filter Photographs of the Inter-electrode Region.

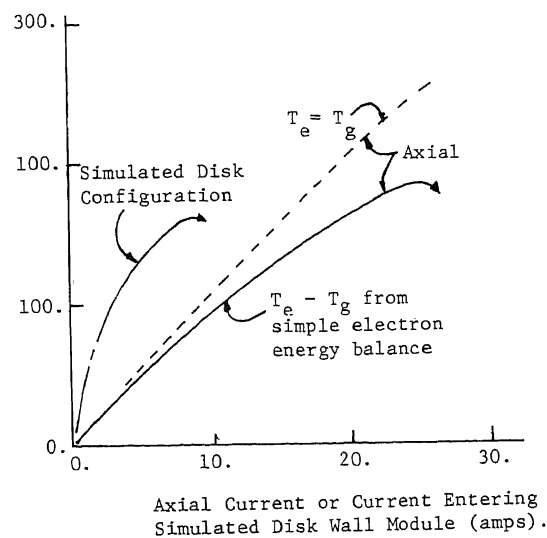


Figure 8 Voltage-Current Calculations for axial and simulated disk configurations.